

Neale, and H. L. Ravn, *Z. Naturforsch.* **21a**, 1042 (1966).

<sup>8</sup>S. O. Thompson, L. Husain, and S. Katcoff, *Phys. Rev. C* **3**, 1538 (1971).

<sup>9</sup>J. Hudis and S. Katcoff, *Phys. Rev.* **180**, 1122 (1969).

<sup>10</sup>R. Brandt, F. Carbonara, E. Cieslak, H. Piekartz, J. Piekartz, and J. Zakrzewski, private communication.

<sup>11</sup>G. Remy, J. Ralarosy, R. Stein, M. Debeauvais, and J. Tripier, private communication.

<sup>12</sup>R. Brandt, E. Carbonara, E. Cieslak, I. Jarstorff, J. Piekartz, R. Rinziivillo, and J. Zakrzewski, *J. Phys. (Paris)* **31**, 21 (1970).

<sup>13</sup>E. K. Hyde, *The Nuclear Properties of the Heavy Elements* (Prentice-Hall, Inc., Englewood Cliffs, New Jersey, 1964), Vol. III, pp. 481-485.

<sup>14</sup>B. Budick, S. C. Cheng, E. R. Macagno, A. M. Rush-ton, and C. S. Wu, *Phys. Rev. Letters* **24**, 604 (1970).

<sup>15</sup>J. B. Cumming, G. Friedlander, and S. Katcoff,

*Phys. Rev.* **125**, 2078 (1962).

<sup>16</sup>L. E. Agnew, O. Chamberlain, D. V. Keller, R. Mermond, E. H. Rogers, H. M. Steiner, and C. Wiegand, *Phys. Rev.* **108**, 1545 (1957).

<sup>17</sup>W. Galbraith, E. W. Jenkins, T. F. Kycia, B. A. Leontic, R. H. Phillips, A. L. Read, and R. Rubinstein, Brookhaven National Laboratory Report No. BNL-11598, 1967 (unpublished).

<sup>18</sup>R. J. Abrams, R. L. Cool, G. Giacomelli, T. F. Kycia, B. A. Leontic, K. K. Li, A. Lundby, D. N. Michael, and J. Teiger, private communication.

<sup>19</sup>T. Coor, D. A. Hill, W. F. Hornyak, L. W. Smith, and G. Snow, *Phys. Rev.* **98**, 1369 (1955).

<sup>20</sup>G. Bellettini, G. Cocconi, A. N. Diddens, E. Lillethun, G. Matthiae, J. P. Scanlon, and A. M. Wetherell, *Nucl. Phys.* **79**, 609 (1966).

<sup>21</sup>See Hyde, Ref. 13, pp. 380-387.

## Effect of Pu<sup>240</sup> Compound-Nucleus State on the Fission-Fragment Mass and Kinetic Energy Distributions\*

Jayashree Toraskar and E. Melkonian

*Columbia University, New York, New York 10027*

(Received 7 October 1970)

Fission-fragment mass and kinetic energy distributions have been obtained for fission of Pu<sup>239</sup> induced by neutrons filtered through beryllium and by neutrons filtered through samarium. The beryllium filter enhances the contribution of the negative-energy resonance level to the fission cross section, and the samarium filter enhances the contribution of the 0.297-eV level. Surface-barrier detectors were used for the simultaneous measurement of both the fragment energies. Absolute fragment energies were calculated by using mass-dependent pulse-height energy relations.

The average total kinetic energy of the fragments produced in the fission induced by samarium-filtered neutrons was observed to be  $0.75 \pm 0.05$  MeV greater than in the case of fission induced by beryllium-filtered neutrons. This result, when combined with the results of other experiments, implies  $J=0^+$  for the negative-energy level and  $J=1^+$  for the 0.297-eV level of Pu<sup>239</sup>. The two mass distributions are similar except for a difference in the symmetric fission yield. This difference again implies the same spin assignments as above. The absolute average total kinetic energies were determined with somewhat less accuracy and are found to be  $173.0 \pm 1.5$  and  $173.7 \pm 1.5$  MeV for fissions induced by beryllium- and samarium-filtered neutrons, respectively, as directly measured, and  $175.8 \pm 1.5$  and  $176.5 \pm 1.5$  MeV, respectively, after correction for neutron emission.

### INTRODUCTION

It is well accepted that the symmetric-to-asymmetric fission ratio varies with the excitation energy of the compound nucleus. It was suggested by Wheeler<sup>1</sup> that this ratio should also be different for the two possible spin states of the compound nucleus formed by the addition of a neutron to the nucleus. Experimental evidence of such a variation has been found in the cases of low-energy neutron-induced fission of U<sup>233</sup>, U<sup>235</sup>, and Pu<sup>239</sup>. Radiochemical measurements of Regier *et al.*<sup>2</sup> indicate that this ratio is 5.3 times larger for one

of the two spin states that can be formed by addition of a thermal neutron to the Pu<sup>239</sup> nucleus. Walter, Neiler, and Schmitt (WNS)<sup>3</sup> have confirmed this large variation for Pu<sup>239</sup> by double energy measurements of the fission fragments. However, they did not investigate the effect of the compound-nucleus state on the corresponding energy distributions. Melkonian and Mehta<sup>4</sup> have investigated the variation of average kinetic energy of one fragment in the resonance-neutron-induced fission of U<sup>235</sup> and Pu<sup>239</sup> and have found correlation between the average kinetic energy and the spin of the resonance level.

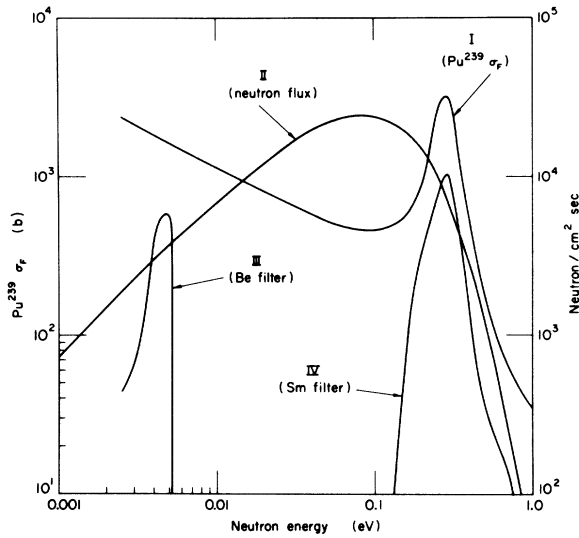


FIG. 1. Neutron fission cross section of  $Pu^{239}$  (curve I), neutron flux distribution (curve II), and the resulting fission yields when 10 in. of beryllium (curve III) or 30 mil of samarium is inserted in the neutron beam. The units for curve III and curve IV are arbitrary.

In the present study, the total kinetic energy and mass distributions for the fission of  $Pu^{239}$  induced by neutrons filtered through 0.03 in. of

samarium and by neutrons filtered through 10 in. of liquid-nitrogen-cooled crystalline beryllium are investigated. Figure 1 shows the neutron fission cross section of  $Pu^{239}$  and the approximate neutron flux distribution over the energy range 0.001–1.0 eV. Also shown are the resulting fission yields as function of energy when 10 in. of beryllium or 30 mil of samarium is inserted in the neutron beam. About 80% of the fission events measured with the samarium filter were estimated to be from the 0.297-eV level. The beryllium filter transmits neutrons of energy below 0.0052 eV and therefore increases the contribution of the negative-energy level to the fission process. These two neutron resonances of  $Pu^{239}$  are believed to have opposite spins ( $0^+$  and  $1^+$ ).

EXPERIMENTAL METHOD

An enriched  $Pu^{239}$  (99.5%) target prepared by vacuum evaporation of plutonium fluoride onto a 5- $\mu$ m-thick nickel foil was used. The thickness of the deposit was about 18  $\mu$ g/cm<sup>2</sup> on an area of about 150 mm<sup>2</sup>.

A neutron beam from the Brookhaven Graphite Research Reactor was collimated so that it did not strike the detectors directly. The detectors

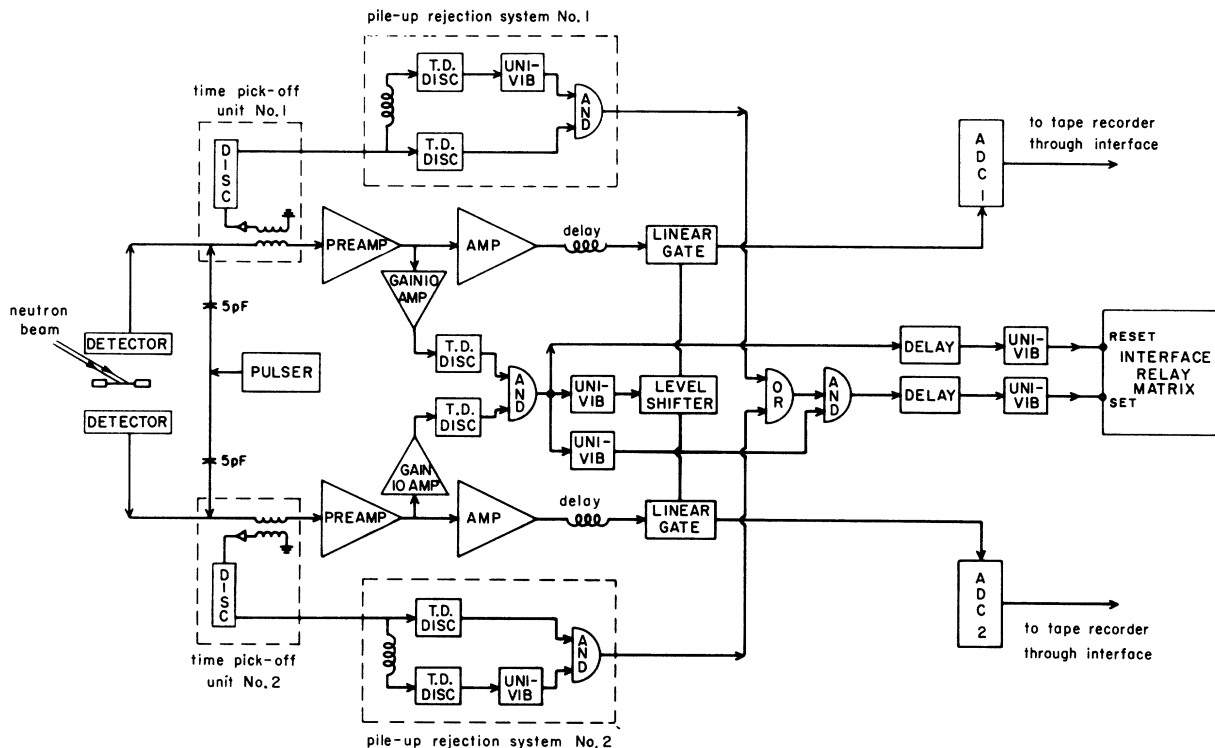


FIG. 2. Schematic diagram of source and detector arrangement and the block diagram of the electronics used in the present experiment.

were of the heavy-ion surface-barrier type with active area of  $\sim 4 \text{ cm}^2$ . Aluminum masks,  $\frac{1}{16}$  in. thick with rounded-edge apertures slightly smaller than the sensitive area of the detectors, were used to prevent detection of the fragments with degraded energies arising from edge effects in the detectors.

Figure 2 shows the block diagram of the electronics used together with the schematic arrangement of the detectors and target. The electronic system consisted of two similar systems for energy measurements (one for each detector) and two similar systems for  $\alpha$ -particle pileup rejection. At the output of the detector, a time pickoff unit divided the signal into two parts as shown in the block diagram. The main part of the detector signal went through the primary of the transformer in the time pick-off unit and then to a charge-sensitive preamplifier. The output of the preamplifier was further amplified by a double-delay-line (DDL) amplifier. The choice of a DDL amplifier was made particularly to reduce the effects of the large  $\alpha$  pileup. The output from the coincidence circuit (resolving time  $\approx 100 \text{ nsec}$ ) opened the linear gates for about  $0.6 \mu\text{sec}$  (clipping time of the DDL amplifiers used). The signals from the linear gates were fed directly into the two-parameter data-acquisition system. A conversion of 1000 channels full scale was used, giving  $\approx 0.2 \text{ MeV}$  per channel. Pulsar signals were fed through a small capacitance ( $\approx 5 \text{ pF}$ ) into the time pick-off unit at the same point where the detector signals came in. These signals were used for checking the stability and linearity of the whole system.

The fast-rising and narrow output from the secondary of the time pickoff transformer was fed into the pileup rejection system. The system gave an output pulse whenever two input pulses were

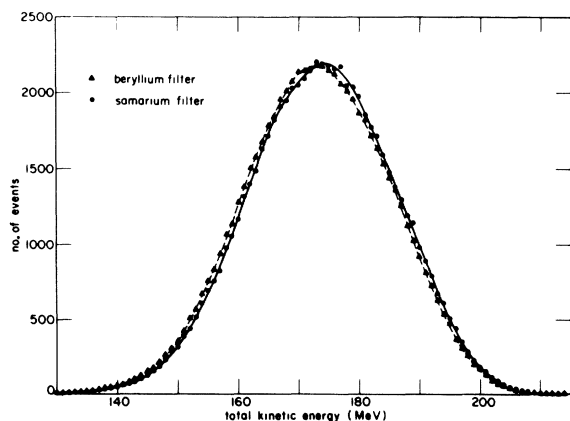


FIG. 3. Measured total kinetic energy distributions for the  $\text{Pu}^{239}$  fissions induced by the beryllium- and samarium-filtered neutrons.

separated by a time interval  $t$  such that  $T_L < t < T_U$  ( $T_L = 100 \text{ nsec}$  and  $T_U = 1.2 \mu\text{sec}$ ). This pileup information was recorded onto magnetic tape simultaneously with the pulse-height information for that event. During the analysis of the data, those events which had pileup were rejected before calculating the mass and energy distributions.

About 197 000 events were collected for the epismarium neutron-induced fission. 410 000 events were recorded with the beryllium filter. Data were also collected for fission induced by unfiltered neutrons, and were used for calibrating the detectors.

#### DATA ANALYSIS

The measured pulse heights are linear functions of the fragment energies after neutron emission. No exact energy and momentum conservation relations can be used without considering the neutron emission from each fragment. We have used the following approximate relations to analyze the data:

$$\mu_1 E_1 = \mu_2 E_2, \quad (1)$$

$$\mu_1 + \mu_2 = A, \quad (2)$$

$$E_1 + E_2 = E_K, \quad (3)$$

where  $\mu_1$  and  $\mu_2$  are some intermediate masses,  $E_1$  and  $E_2$  are the kinetic energies of the two complementary fragments, and  $E_K$  is the total kinetic energy released in the fission event. The energy and mass distributions so obtained were then cor-

TABLE I. Properties of the measured kinetic energy distributions and the intermediate mass distributions. All errors are statistical. All energies are in MeV and masses in amu.

Quantity	Induced fission of $\text{Pu}^{239}$	
	Beryllium-filtered neutrons (type I)	Samarium-filtered neutrons (type II)
$\langle \mu_L \rangle^a$	$100.27 \pm 0.02$	$100.39 \pm 0.02$
$\langle \mu_H \rangle^b$	$139.49 \pm 0.02$	$139.75 \pm 0.02$
$\langle E_L \rangle^c$	$100.66 \pm 0.01$	$100.99 \pm 0.02$
$\langle E_H \rangle^d$	$72.32 \pm 0.02$	$72.72 \pm 0.03$
$\langle E_K \rangle^e$	$172.98 \pm 0.02$	$173.71 \pm 0.04$
$\sigma(E_K)^f$	12.13	12.13
$\sigma(\mu_L)^g$	6.79	6.86
$\sigma(\mu_H)^h$	6.79	6.85

<sup>a</sup>Average mass of the light fission fragment.

<sup>b</sup>Average mass of the heavy fission fragment.

<sup>c</sup>Average kinetic energy of the light fragment.

<sup>d</sup>Average kinetic energy of the heavy fragment.

<sup>e</sup>Average total kinetic energy.

<sup>f</sup>rms width of the total kinetic energy distribution.

<sup>g</sup>rms width of the light-fragment mass distribution.

<sup>h</sup>rms width of the heavy-fragment mass distribution.

TABLE II. Average values and the rms widths of the pre-neutron-emission energy and mass distributions. All energies are in MeV and masses in amu; all errors are combinations of statistical and calibration errors.

Quantity	Induced fission of Pu <sup>239</sup>	
	Beryllium-filtered neutrons (type I)	Samarium-filtered neutrons (type II)
$\langle E_L^* \rangle$	102.1 ± 1.2	102.4 ± 1.2
$\langle E_H^* \rangle$	73.7 ± 1.0	74.1 ± 1.0
$\langle E_K^* \rangle$	175.8 ± 1.5	176.6 ± 1.5
$\langle m_L^* \rangle$	100.6 ± 1.0	100.7 ± 1.0
$\langle m_H^* \rangle$	139.1 ± 1.0	139.3 ± 1.1
$\sigma(m_L^*)$	5.81	5.77
$\sigma(m_H^*)$	5.81	5.77

rected for the neutron emission by the method described by Schmitt, Neiler, and Walter<sup>5</sup> to get the pre-neutron-emission distributions.

### RESULTS

The measured total kinetic energy distribution  $N(E_K)$  for the fission by neutrons filtered through beryllium crystal (type I) is shown superimposed on that corresponding to fission by episamarium neutrons (type II) in Fig. 3. There is a significant displacement of one distribution with respect to the other; however, the general shapes of the two distributions appear to be similar otherwise. The average single fragment energies show shifts in the same direction as the total kinetic energies. Table I gives the various average energies and other related quantities for the two types of induced fission studied. All the measurements were done under similar conditions so that the systematic errors are unimportant for comparison purposes. The errors given in Table I are statistical errors. Table II gives the various average pre-neutron-emission quantities. The errors in Table

II are the absolute errors of the measurements. It was assumed that the neutron emission from the fragments remains the same for the two types of induced fission studied. Data of Apalin *et al.*<sup>6</sup> on the neutron-induced fission of Pu<sup>239</sup> were used for the correction. Table III gives the distribution of events as a function of total kinetic energy for the two cases. The type-I fission has more events in the lower kinetic energy regions which results in lower average total kinetic energy than that for the type-II case.

Figures 4(a) and 4(b) show the intermediate mass distributions  $N(\mu)$  for the two cases. The corresponding pre-neutron-emission distributions  $N(m^*)$  are shown superimposed on  $N(\mu)$  for each case in Figs. 5(a) and 5(b). The two mass distributions differ significantly only in the symmetric mass region. This is more evident from Figs. 6(a) and 6(b) where the fission yields in the symmetric and the most asymmetric mass regions are plotted. As there are very few counts in the asymmetric region, the mass distributions were reflected around mass 120 and the resultant distributions were used to draw Fig. 6(b). The yields for type-II fission in the asymmetric mass region are systematically higher than those for type-I fission, however this increase in yields is very small and is not so evident in the total (summed over all kinetic energies) mass distributions. The asymmetric-to-symmetric fission yield ratio calculated from the pre-neutron-emission mass distributions are  $106 \pm 11$  for the type-I fission (beryllium filter) and  $185 \pm 25$  for the type-II fission (samarium filter).

### DISCUSSION

The variation of the asymmetric-to-symmetric ratio for type-I and type-II fission agrees qualitatively with the results of WNS<sup>3</sup> and of Regier

TABLE III. Distribution of events as a function of total kinetic energy  $E_K$ .

$E_K$ (MeV)	Induced fission of Pu <sup>239</sup>		$\frac{\text{Events in type-II fission}}{\text{Events in type-I fission}}$
	Beryllium-filtered neutrons (type I) (fraction of total events)	Samarium-filtered neutrons (type II) (fraction of total events)	
152.5	0.0414	0.0371	0.8961
157.5	0.0762	0.0695	0.9126
162.5	0.1180	0.1111	0.9419
167.5	0.1506	0.1470	0.9757
172.5	0.1657	0.1649	0.9634
177.5	0.1560	0.1610	1.0321
182.5	0.1274	0.1322	1.0375
187.5	0.0911	0.0952	1.0448
192.5	0.0519	0.0572	1.0916
197.5	0.0218	0.0248	1.1380

*et al.*<sup>2</sup> Our results indicate that the asymmetric-to-symmetric fission ratio for type-I fission is  $1.74 \pm 0.30$  times smaller than for type-II fission. WNS<sup>3</sup> find the value of  $2.0 \pm 0.4$  for the same ratio from the simultaneous energy measurements of the fission fragments. Radiochemical measurements of Regier *et al.*<sup>2</sup> give a value of  $2.34 \pm 0.06$  for the  $\text{Mo}^{99}/\text{Sn}^{121}$  yield ratio. The disagreement of the latter result with the results obtained from the energy measurements may be due to different types of mass distribution used to determine the ratio. Their results were obtained by measuring the yields of particular nuclei in the post-neutron mass distribution. Our calculations are based on the pre-neutron mass distributions. Neutron emission changes the region of symmetric mass division considerably, while the region of maximum yields is affected only slightly. Since the yields in the symmetric region are very small, even a small change in these yields changes the peak-to-valley ratio considerably, and the comparison of the radiochemical and physical measurements may not be justified. Recent measurements on the neutron multiplicities<sup>7,8</sup> for the resonance-neutron-induced fission of  $\text{Pu}^{239}$  indicate correlation with the spin of the level. It is also possible that the shapes of the neutron distribution  $\nu(\mu)$  for the two spin states are different and the assumption that the  $\nu(\mu)$  remains unchanged for the both

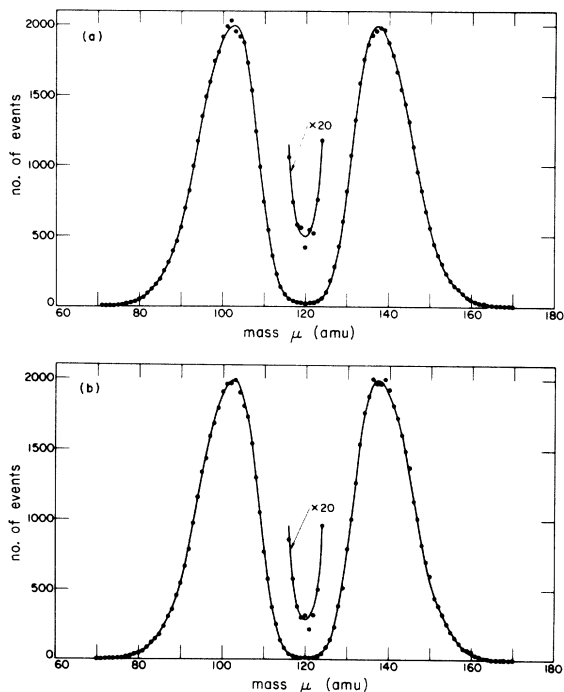


FIG. 4. Mass distributions  $N(\mu)$  for the  $\text{Pu}^{239}$  fissions induced by (a) the beryllium-filtered neutrons and (b) the samarium-filtered neutrons.

types of fission, made to calculate the pre-neutron distributions in the present measurements, may not be correct.

Figure 6(b) indicates that the yields in the asymmetric region are generally larger for type-II fission than those for type I, for each kinetic energy slice. However, in the total mass distributions, this effect is not evident and the yields for the two types of fission agree within statistical errors. Croall and Willis<sup>9</sup> have investigated the thermal- and epithermal-neutron-induced fission of  $\text{Pu}^{239}$ . Their results indicate that a decrease in the symmetric fission yield is accompanied by a significant increase in yield for very asymmetric fission, particularly for  $\text{As}^{77}$  and  $\text{As}^{78}$ . Again one should remember that these measurements are radiochemical and hence give the yields for the post-neutron mass distribution rather than the pre-neutron one as is obtained from energy measurements.

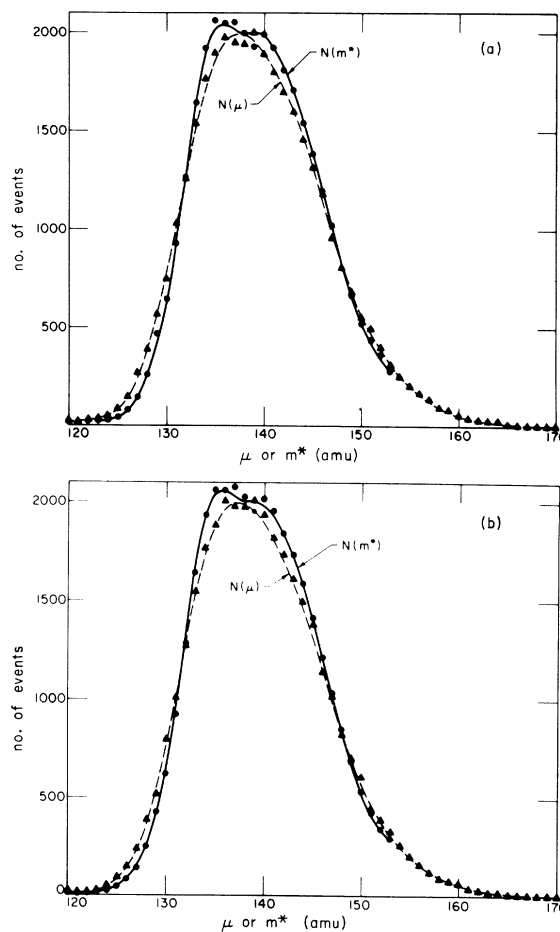


FIG. 5. Mass distributions  $N(\mu)$  and the corresponding pre-neutron-emission mass distributions  $N(m^*)$  for the  $\text{Pu}^{239}$  fissions induced by (a) the beryllium-filtered neutrons and (b) the samarium-filtered neutrons.

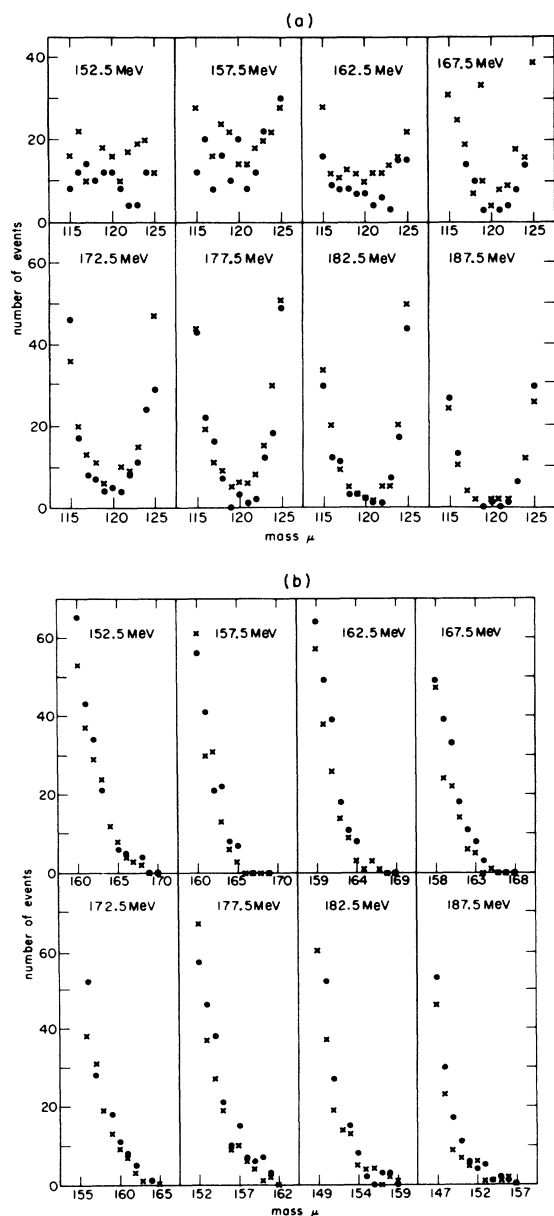


FIG. 6. Normalized yields for the type-I and type-II fissions as functions of total kinetic energy. (a) Yields in the symmetric mass region for the type-I (crosses) and the type-II (solid circles), (b) yields in the highly asymmetric mass region for the type-I (crosses) and the type-II (solid circles) fissions [(b) was drawn after reflecting the mass distributions about mass 120].

The spin of the negative-energy level and the 0.297-eV level of  $\text{Pu}^{239}$  have not been measured directly. The variation of asymmetric-to-sym-

metric fission yield ratios for resonances between 15 and 80 eV<sup>10</sup> combined with the results of Regier *et al.*<sup>2</sup> for these two levels indicate that the 0.297-eV level and the negative level have spins  $1^+$  and  $0^+$ , respectively. Our results on the yields in the symmetric region are consistent with these spin assignments.

The correlation between the average kinetic energy and the spin of the level found by Melkonian and Mehta<sup>4</sup> predicts lower kinetic energy for the  $0^+$  levels. The results of the present experiment help to confirm this correlation.

Contradictory correlations<sup>7,8</sup> have been found between the neutron multiplicities and the spins of the individual resonances in the resonance-neutron-induced fission of  $\text{Pu}^{239}$ . These correlations would imply slightly different internal excitation energies for the negative-energy and 0.297-eV levels. The smaller kinetic energy for the  $0^+$  level found in the present measurements is consistent with the measurements of Weinstein and Block<sup>7</sup> which indicate that the average multiplicity for the  $J=0^+$  group is 2.6% higher (i.e., 0.08 neutrons more) than for the  $J=1^+$  group. By assuming that the average number of neutrons emitted per fission increases by 0.12 neutrons/MeV of excitation energy, they predict that the observed difference in the average number of neutrons corresponds to 0.7 MeV more internal excitation energy for the  $J=0^+$  state than  $J=1^+$  state. If we further assume that the average  $\gamma$  emission does not change significantly with the spin state, this implies that about 0.7 MeV less kinetic energy should be observed for fission from  $J=0^+$  states than the  $J=1^+$  state. This value agrees very well with the 0.75-MeV kinetic energy difference observed in this experiment.

In conclusion, the present measurements indicate that the average kinetic energies as well as the symmetric fission yields are dependent on the spin state of the fissioning nucleus.

#### ACKNOWLEDGMENTS

The authors wish to thank the staff of the Brookhaven Graphite Research Reactor for their assistance during the experiment. The authors are grateful to Dr. E. H. Kobisk of Oak Ridge National Laboratory for the preparation of the targets. The interest and help given by Dr. Mary Derengowski and Dr. Ivan G. Schroeder throughout this work is gratefully acknowledged.

\*Work supported in part by the U. S. Atomic Energy Commission.

<sup>1</sup>J. A. Wheeler, *Physica* **22**, 1103 (1965).

<sup>2</sup>R. B. Regier, W. H. Burgus, R. L. Tromp, and B. H. Sorenson, *Phys. Rev.* **119**, 2017 (1960).

<sup>3</sup>F. J. Walter, J. H. Neiler, and H. W. Schmitt, *Bull.*

Am. Phys. Soc. 8, 369 (1963).

<sup>4</sup>E. Melkonian and G. K. Mehta, in *Proceedings of the Symposium on the Physics and Chemistry of Fission, Salzburg, 1965* (International Atomic Energy Agency, Vienna, Austria, 1965), Vol. II, p. 355.

<sup>5</sup>H. W. Schmitt, J. H. Neiler, and F. J. Walter, *Phys. Rev.* **141**, 1146 (1966).

<sup>6</sup>V. F. Apalin, Y. N. Gritsyuk, I. E. Kutikov, V. I. Levedev, and L. A. Mikaelian, *Nucl. Phys.* **71**, 553 (1965).

<sup>7</sup>S. Weinstein and R. C. Block, *Phys. Rev. Letters* **22**, 195 (1969).

<sup>8</sup>Y. V. Ryabov, in *Proceedings of the Second International Atomic Energy Symposium on Physics and Chemistry of Fission, Vienna, Austria, 1969* (International Atomic Energy Agency, Vienna, Austria, 1969), p. 486.

<sup>9</sup>I. F. Croall and H. H. Willis, in *Proceedings of the Symposium on the Physics and Chemistry of Fission, Salzburg, 1965* (International Atomic Energy Agency, Vienna, Austria, 1965), Vol. I, p. 355.

<sup>10</sup>G. A. Cowan, B. P. Bayhurst, R. J. Prestwood, J. S. Gilmore, and G. W. Knobeloch, *Phys. Rev.* **144**, 979 (1966).

PHYSICAL REVIEW C

VOLUME 4, NUMBER 1

JULY 1971

## Neutron-Induced Fission Cross Section of <sup>252</sup>Cf†

M. S. Moore and J. H. McNally

*Los Alamos Scientific Laboratory, University of California, Los Alamos, New Mexico 87544*

and

R. D. Baybarz

*Oak Ridge National Laboratory, Oak Ridge, Tennessee 37830*

(Received 5 April 1971)

The neutron-induced fission cross section of <sup>252</sup>Cf was measured from 20-eV to 5-MeV neutron energy, using neutrons from the Physics-8 nuclear explosion. Pronounced sub-barrier resonance fission is observed below a few keV neutron energy. The fission threshold is found to occur at ~900 keV. Analysis of the data indicates that the fission barrier is quite transparent, giving an average fission width comparable to the value of 0.02–0.05 eV expected for the average radiative capture width in the resonance region.

The nuclear explosion as a neutron source is unique for the measurement of neutron cross sections of highly radioactive nuclei, since the signal-to-noise ratio is so high that the natural radioactivity of the sample is completely negligible. During the Physics-8 nuclear explosion, a sample of 60 μg of <sup>252</sup>Cf was placed in the neutron beam. The spontaneous-fission rate of this sample was high by usual standards (about 10<sup>8</sup> fragments/sec being emitted), but posed no problem for the fission-cross-section measurement by this technique.

The <sup>252</sup>Cf fission foil was prepared at the Oak Ridge National Laboratory (ORNL) by electro-deposition from an organic solvent<sup>1</sup> onto a stainless-steel backing, 3.5 × 10<sup>-3</sup> mm thick. The deposit was coated with a thin layer of nickel (~5 × 10<sup>-6</sup> cm), to minimize evaporation of the material from the surface by spontaneous-fission heating. After fabrication, the fission foil was mounted in a specially designed shipping cask from which it could be positioned remotely into the neutron beam at the time of the experiment. The foil was assayed both at ORNL and at the Los Alamos Scientific Laboratory (LASL) by low-geometry counting. At LASL, the energy deposited per fission was

also determined by measuring the pulse-height spectrum of fragments of spontaneous fission incident on a solid-state detector typical of those used in the actual measurement. The isotopic composition of the sample, at the time the measurement took place, was as follows: <sup>248</sup>Cm, 10.1%; <sup>249</sup>Cf, 0.03%; <sup>250</sup>Cf, 0.66%; <sup>251</sup>Cf, 0.17%; <sup>252</sup>Cf, 89.0%; <sup>253</sup>Cf, 0.01%; <sup>254</sup>Cf, 0.03%. (The sample was greater than 99% <sup>252</sup>Cf, as far as Cf isotopes were concerned. The major contaminant, <sup>248</sup>Cm, originated from <sup>252</sup>Cf decay between the time of sample purification and the experiment.)

Data recording and data reduction were carried out in a way which has been previously described.<sup>2</sup> The fission cross section of <sup>252</sup>Cf was determined relative to the cross section of <sup>6</sup>Li(*n*, *t*)<sup>4</sup>He below 100 keV,<sup>3</sup> and relative to the <sup>235</sup>U fission cross section<sup>4</sup> above 100 keV. The data also required a renormalization. Based on the isotopic analysis given above, it was observed that the apparent contribution of <sup>248</sup>Cm fission in the 76- and 99-eV resonances was a factor of 5.0 too low. It was concluded that the alignment of the sample in the neutron beam was at fault. The renormalization by a factor of 5 is discussed in detail in the Appendix;